Phenomenological and microscopic model analysis of elastic scattering reactions of ^{18}O by ^{24}Mg, ^{28}Si, ^{58}Ni, ^{64}Zn, ^{90}Zr, ^{120}Sn, and ^{208}Pb target nuclei

M. Aygun[a], O. Kocadag[b], and Y. Sahin[b]
[a] *Department of Physics, Bitlis Eren University, Bitlis, Turkey.*
[b] *Department of Physics, Ataturk University, Erzurum, Turkey.*

Received 16 June 2015; accepted 30 July 2015

In the present study, the optical potentials are obtained to describe the interactions of ^{18}O at different incident energies. With this goal, the elastic scattering angular distribution data measured for many systems, ranging from ^{24}Mg to ^{208}Pb are analyzed by using the phenomenological model (PM) and the double folding model (DFM) within the framework of optical model (OM). It is presented that the theoretical results with the PM and the DFM are in very good agreement with both the experimental data and the results of previous studies. A new global set of imaginary potential of the double folding calculations is derived to describe the interactions of ^{18}O at low energies. Also, the volume integrals of potentials, the cross sections and χ^2/N values obtained by means of the theoretical calculations for each system are given.

Keywords: Optical model; elastic scattering.

PACS: 24.10.Ht; 24.50.+g; 25.70.-z

1. Introduction

The nuclear reactions are from the most important topics of nuclear physics. When two or more particles collide at any energy, the different forms of nuclear reactions such as elastic scattering, inelastic scattering, transfer reactions, breakup reactions, etc. may occur [1]. The elastic scattering is the most common type of reactions. In this process, the total kinetic energy of system is conserved in the center-of-mass frame. The angular distribution of elastic scattering for any reaction is investigated via different theoretical approaches. The optical model (OM) is accepted as one of the simplest and the most successful models of nuclear physics in the explanation the elastic scattering. In this context, the phenomenological model (PM) and the double folding model (DFM) within the framework of OM are among the most well known models. In the phenomenological formalism, Woods-Saxon (WS) shaped potential for the real and the imaginary parts of optical potential is often applied. However, the DFM determines the real potential over the density distributions of projectile nucleus and target nucleus [2–5].

There have been many experimental efforts to study the interactions with ^{18}O [6–11]. Some of these experiments have been on the elastic scattering of projectile ^{18}O by several target nuclei at different incident energies. They have been analyzed by using different theoretical approaches. Bernas *et al*. [12] measured the elastic and the inelastic scattering data of ^{18}O + ^{24}Mg system at $E_{\rm lab} = 50$ MeV and also gave the theoretical results as compared with the experimental data. Mermaz *et al*. [13] reported the elastic scattering data as well as the inelastic scattering data of projectile ^{18}O scattered from ^{28}Si target nucleus at incident energy of 56 MeV. They performed the theoretical analysis via the OM and the coupled-channels (CC) approach. Alves *et al*. [14] measured the experimental data of elastic scattering of ^{18}O by ^{58}Ni at $E_{\rm lab} = 46$ MeV. They presented the results of theoretical analysis of the data. Salém-Vasconcelos *et al*. [15] recorded the elastic and the inelastic scattering of ^{16,18}O + ^{64}Zn systems at $E_{\rm lab} = 49$ MeV. They showed the agreement between the theoretical results based on the OM and the experimental data. Also, they observed a sharp difference by means of the inelastic ^{64}Zn (2^+) excitation function for both ^{16}O and ^{18}O nuclei. As a reason of this, they indicated that the two neutrons of ^{18}O contribute to the nuclear interaction. Jha *et al*. [16] studied as compared the two systems ^{16}O + ^{90}Zr and ^{18}O + ^{90}Zr. With this goal, they measured the elastic scattering angular distribution at 90 MeV and reported that the two neutrons of ^{18}O do not show an important effect on both the elastic scattering data and the optical potential according to ^{16}O + ^{90}Zr. Robertson *et al*. [17] measured the elastic scattering data for ^{18}O + ^{120}Sn system at $E_{\rm cm} = 57.97$ MeV. They performed the analysis of data by using the OM. Vulgaris *et al*. [18] measured fusion, transfer, and elastic scattering for ^{16,18}O + ^{208}Pb systems. Consequently, a large body of experimental data at various incident energies has been accumulated for the elastic scattering of ^{18}O nucleus with different target nuclei. However, we need further theoretical study in order to better understand the experimental data of the reactions regarding ^{18}O nucleus. For example, a global OM parameters are necessary to determine the inelastic scattering and the quasielastic scattering of the system investigated by means of the CC formalism or to use in the calculations of transfer reactions. But, if one researches the global potential parameters for these systems in the literature, one can not obtain them. In addition to this, there is no the theoretical analysis of PM and DFM reported in the literature, which the similarities and differences of the models used in analysis with this comparison are pleasantly visible. The present study has been divided into two parts. We first obtain the potential parameters of elastic scattering angular distributions

of ^{18}O-nucleus reactions by using the PM. Then, we find the global potential parameters of the same reactions with the aid of DFM. We reacquire the theoretical results reported in previous studies and compare these results with the PM and the DFM results as well as the experimental data. The similarities and differences between the models used in the calculations are provided.

In the next section, we present the theoretical model used in our calculations. The results of these calculations are presented in Sec. 3. Section 4 is devoted to our conclusions.

2. Theoretical Analysis

The elastic scattering data of ^{18}O by ^{24}Mg, ^{28}Si, ^{58}Ni, ^{64}Zn, ^{90}Zr, ^{120}Sn, and ^{208}Pb target nuclei at different incident energies are investigated. Thus, a comprehensive analysis over various target nuclei and different theoretical models is carried out. For this, it is assumed that the theoretical calculations consist of the two parts which are the PM and the DFM within the framework of OM.

The total potential over the potentials describing the system investigated is given by

$$V_{\text{total}}(r) = V(r) + iW(r) + V_{\text{C}}(r), \tag{1}$$

where $V(r)$ and $iW(r)$ are the real part and the imaginary part of nuclear potential, respectively. $V_{\text{C}}(r)$ denotes the Coulomb potential taken as [19]

$$V_{\text{C}}(r) = \frac{1}{4\pi\epsilon_\circ}\frac{Z_P Z_T e^2}{r}, \qquad r \geq R_c \tag{2}$$

$$= \frac{1}{4\pi\epsilon_\circ}\frac{Z_P Z_T e^2}{2R_c}\left(3 - \frac{r^2}{R_c^2}\right), \qquad r < R_c \tag{3}$$

where R_c is the Coulomb radius, taken as $1.25(A_P^{1/3} + A_T^{1/3})$ fm in the calculations and Z_P and Z_T present the charges of the projectile P and the target nuclei T, respectively.

2.1. Phenomenological Model Analysis

Here our aim is to obtain the potential parameters for the same potential geometry of all the reactions investigated with the aid of phenomenological analysis. In this context, the real part and the imaginary part of the nuclear potential are chosen as WS shaped potential. In this way, the nuclear potential is written in the following form

$$V_{\text{Nuclear}}(r) = -\frac{V_0}{1 + \exp(\frac{r - r_v\,(A_P^{1/3} + A_T^{1/3})}{a_v})} - \frac{W_0}{1 + \exp(\frac{r - r_w\,(A_P^{1/3} + A_T^{1/3})}{a_w})}, \tag{4}$$

where A_P and A_T are the masses of projectile and target nuclei, respectively. The parameters of the real and the imaginary potentials are obtained by searching of the values which fits the experimental data. This procedure is described below.

2.2. Double Folding Model Analysis

The DFM is often a model used in the determination the real part of nuclear potential. This potential is called the double folding potential in the literature. To obtain the double folding potential in the theoretical calculations, the nuclear matter distributions of both projectile and target nuclei together with an effective nucleon-nucleon interaction potential (ν_{NN}) are used. The double folding potential is given by

$$V_{\text{DF}}(\mathbf{r}) = \int d\overrightarrow{r}_1 \int d\overrightarrow{r}_2 \rho_P \times (\overrightarrow{r}_1)\rho_T(\overrightarrow{r}_2)\nu_{NN}(\overrightarrow{r} - \overrightarrow{r}_1 + \overrightarrow{r}_2), \tag{5}$$

where $\rho_P(\overrightarrow{r}_1)$ and $\rho_T(\overrightarrow{r}_2)$ are the nuclear matter densities of projectile and target nuclei, respectively. In our work, the density distributions of both projectile and target nuclei have been taken from RIPL-3 [20]. In Fig. 1, the density distribution of ^{18}O is displayed. In folding model calculations, we have used the M3Y nucleon-nucleon realistic interaction, which is given by [21]

$$\nu_{NN}(r) = \nu_D(r) + \hat{J}_{00}(E)\delta(r) \tag{6}$$

where $\nu_D(r)$ is the direct part of M3Y interaction and $\hat{J}_{00}(E)$ is the exchange term. $\nu_D(r)$ and $\hat{J}_{00}(E)$, respectively can be expressed as

$$\nu_D(r) = 7999\,\frac{\exp(-4r)}{4r} - 2134\,\frac{\exp(-2.5r)}{2.5r}, \tag{7}$$

$$\hat{J}_{00}(E) \simeq -276\,[1 - 0.005\,(E_{Lab}/A_p)]\ \text{MeV fm}^3. \tag{8}$$

Lastly, the imaginary part of the nuclear potential is taken as WS potential in the following form

$$W(r) = -\frac{W_0}{1 + \exp(\frac{r - r_w\,(A_P^{1/3} + A_T^{1/3})}{a_w})} \tag{9}$$

where A_P and A_T are mass numbers of projectile and target nuclei, respectively.

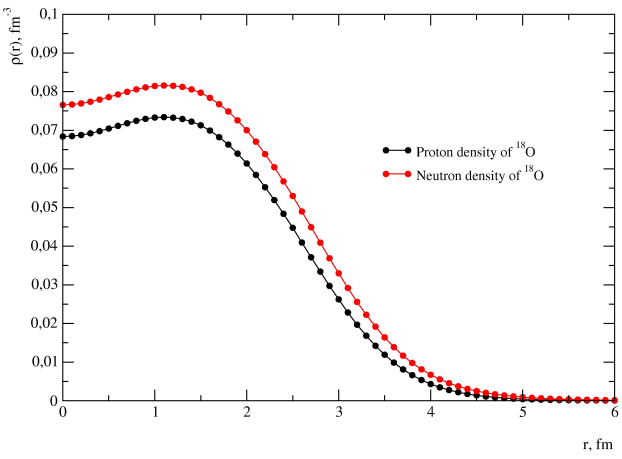

FIGURE 1. The proton and neutron density distributions of ^{18}O nucleus.

TABLE I. The OM parameters used in DFM analysis of ^{18}O scattered from ^{24}Mg, ^{28}Si, ^{58}Ni, ^{64}Zn, ^{90}Zr, ^{120}Sn and ^{208}Pb target nuclei.

System	E_{Lab}	V_0	r_v	a_v	W_0	r_w	a_w	J_v	J_w	σ	$\frac{\chi^2}{N}$
	MeV	MeV	fm	fm	MeV	fm	fm	MeV fm^3	MeV fm^3	mb	
^{18}O+^{24}Mg	50	103	1.110	0.625	28	1.110	0.625	251.4	68.3	1242.9	2.2
^{18}O+^{28}Si	56	90	1.110	0.625	24	1.110	0.625	203.3	54.2	1270.4	2.1
^{18}O+^{58}Ni	46	91.85	1.110	0.625	55	1.110	0.625	148.1	88.7	454.4	0.5
^{18}O+^{64}Zn	49	133	1.110	0.625	70	1.110	0.625	205.6	108.2	618.5	0.2
^{18}O+^{90}Zr	90	80	1.110	0.625	38	1.110	0.625	107.6	51.1	1504.6	1.7
^{18}O+^{120}Sn	66.73	180	1.110	0.625	46	1.110	0.625	217.0	55.4	663.1	1.1
^{18}O+^{208}Pb	86	216	1.110	0.625	105	1.110	0.625	215.1	104.6	475.5	5.2

TABLE II. The OM parameters used in PM analysis of ^{18}O scattered from ^{24}Mg, ^{28}Si, ^{58}Ni, ^{64}Zn, ^{90}Zr, ^{120}Sn and ^{208}Pb target nuclei.

System	E_{Lab}	N_R	W_0	r_w	a_w	J_v	J_w	σ	$\frac{\chi^2}{N}$
	MeV		MeV	fm	fm	MeV.fm^3	MeV.fm^3	mb	
^{18}O+^{24}Mg	50	1.0	20	1.14	0.6	414.2	52.2	1182.8	1.3
^{18}O+^{28}Si	56	1.0	36.5	1.14	0.6	410.2	88.3	1325.4	3.6
^{18}O+^{58}Ni	46	0.83	43	1.14	0.6	344.4	74.5	435.2	0.7
^{18}O+^{64}Zn	49	1.08	43	1.14	0.6	448.1	71.4	574.3	0.8
^{18}O+^{90}Zr	90	0.61	45	1.14	0.6	251.2	65.1	1567.2	1.6
^{18}O+^{120}Sn	66.73	1.0	50	1.14	0.6	413.8	64.9	675.2	1.1
^{18}O+^{208}Pb	86	0.96	61	1.14	0.6	396.2	65.5	413.0	7.1

2.3. Fitting Procedure

In this part, we introduce fitting procedure used while the PM and the DFM calculations are performed. We have first found the values of parameters of real potential and imaginary potential used in the PM calculations. That's why we have started from the values used in the previous studies [12,13,16,17]. We have examined the quality of cohering between the experimental data and the theoretical results of all systems investigated in our study. While the potential parameters have been determined, we have searched the same values of r_v=r_w and a_v=a_w. After we have made the test calculations, we have taken as 1.110 fm the values of r_v=r_w. Then, we have examined the best values of a_v and a_w parameters which give good agreement results with the experimental data for these values fixed of r_v and r_w. We have found 0.625 fm value for a_v=a_w. Finally, we have investigated V_0 and W_0 values for the values obtained of r_v=r_w and a_v=a_w. We have shown the OM parameters obtained for all the reactions in Table I.

Later, the W_0, r_w and a_w values of imaginary potential used in the DFM calculations have been determined as similar to the PM. In this context, firstly, r_w value in steps of 0.1 fm at each incident energy has been investigated and kept constant at 1.14 fm. Then, the a_w value of imaginary potential has been varied in steps of 0.1 and 0.01 fm at the fixed value of r_w and has been taken as 0.6 fm. Finally, the fitting procedure has been completed by adjusting only the depth of imaginary potential. The potential parameters of all the reactions within the framework of DFM are shown in Table II.

The code FRESCO [22] has been used in theoretical calculations of both the PM and the DFM. FRESCO, a general-purpose reaction code, is used in determining the parameters of OM to fit the experimental data.

2.4. Volume Integrals

If one wants to examine the relation between the real and imaginary potentials, one can use the volume integrals of real and imaginary potentials. For this, the volume integral of real potential is determined by using the following formula

$$J_V(E) = \frac{4\pi}{A_P A_T} \int V(r,E) r^2 dr, \tag{10}$$

and for the volume integral of imaginary potential

$$J_W(E) = \frac{4\pi}{A_P A_T} \int W(r,E) r^2 dr, \tag{11}$$

where A_P is the mass number of projectile and A_T is the mass number of target nucleus. The volume integrals for both the real and the imaginary potential have been obtained from the theoretical analysis of elastic scattering data.

2.5. χ^2 Error Calculation

χ^2 error calculation is generally used to discuss the compliance between the theoretical results and the experimental data. With this goal, χ^2 is given in the following form

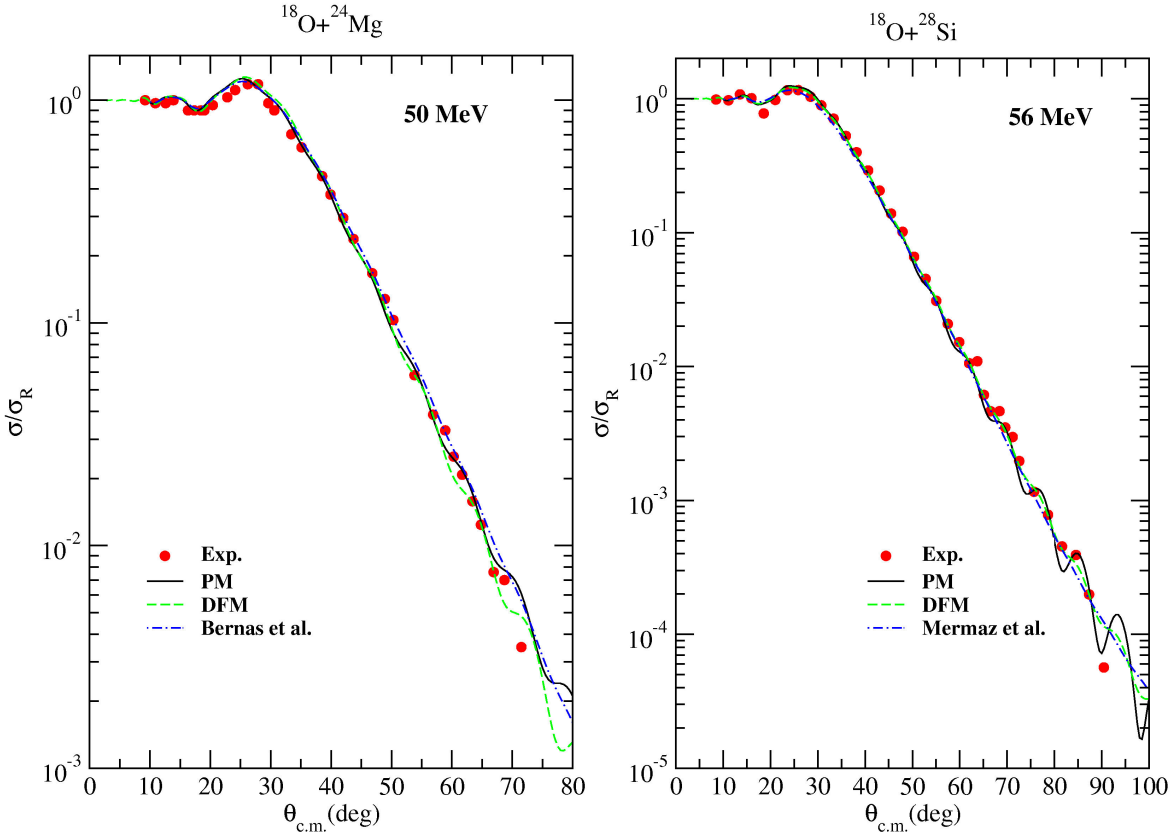

FIGURE 2. The elastic scattering angular distributions for ^{18}O + ^{24}Mg and ^{28}Si. The solid lines show PM results; dashed lines show DFM results and dot-dashed lines show the results obtained by the literature [12, 13]. The circles show the experimental data, which have been taken from [12, 13].

$$\chi^2 = \frac{1}{N}\sum_{i=1}^{N}\frac{(\sigma_{\text{theo}}-\sigma_{\text{exp}})^2}{(\Delta\sigma_{\text{exp}})^2}, \qquad (12)$$

where σ_{theo} is the theoretical cross-section, σ_{exp} is the experimental cross-section, $\Delta\sigma_{exp}$ is the error variation of experimental cross-section and N represents the total number of measured angles.

3. Results and Discussions

We have analyzed the elastic scattering angular distributions of ^{18}O scattered from ^{24}Mg, ^{28}Si, ^{58}Ni, ^{64}Zn, ^{90}Zr, ^{120}Sn and ^{208}Pb target nuclei over different incident energies within the OM. Firstly, we have performed the PM calculations. In order to reduce the number of free parameters of PM, we have sought the convenient values of r_v=r_w and a_v=a_w. We have taken as r_v=r_w=1.11 fm and a_v=a_w=0.65 fm. Then, we have adjusted V_0 and W_0 values and have given all the values of OM parameters in Table I. As seen from Figs. 2, 3 and 4, we can say that the agreement between the PM results and the experimental data is almost perfect. We have compared the PM results with the results of previous studies and have observed that both results are very similar to each other. We have realized that W_0 values are generally large in the PM calculations. This state can be attributed to the efficiency of absorption.

In the second part, we have made the theoretical calculations by using the DFM for the same reactions and the same energies. We have searched the convenient values of r_w and a_w for the same geometry of imaginary potential of systems investigated. We have taken 1.14 fm value for r_w and 0.6 fm value for a_w. For constant values of r_w and a_w, we have determined W_0 values which provide good agreement results with the experimental data. Finally, we have examined the variation of normalization constant (N_R) and have given all the values found in Table II. We have compared the DFM results with the data in Figs. 2, 3 and 4. We have observed that the DFM results are in very good agreement with experimental data as the PM results. In addition, we have presented the DFM results together with the previous studies in Figs. 2, 3 and 4. We have noticed that the DFM results are as good as the results of previous studies.

Figure 5 shows the values of J_v and J_w for the PM and the DFM potentials that fit ^{18}O + ^{24}Mg, ^{18}O + ^{28}Si, ^{18}O + ^{58}Ni, ^{18}O + ^{64}Zn, ^{18}O + ^{90}Zr, ^{18}O + ^{120}Sn, and ^{18}O + ^{208}Pb data. As will be seen, the volume integrals per nucleon pair for the different real potentials present similar behavior. The difference between the magnitudes of real volume integrals is due to the use of folding model with deep potential. The

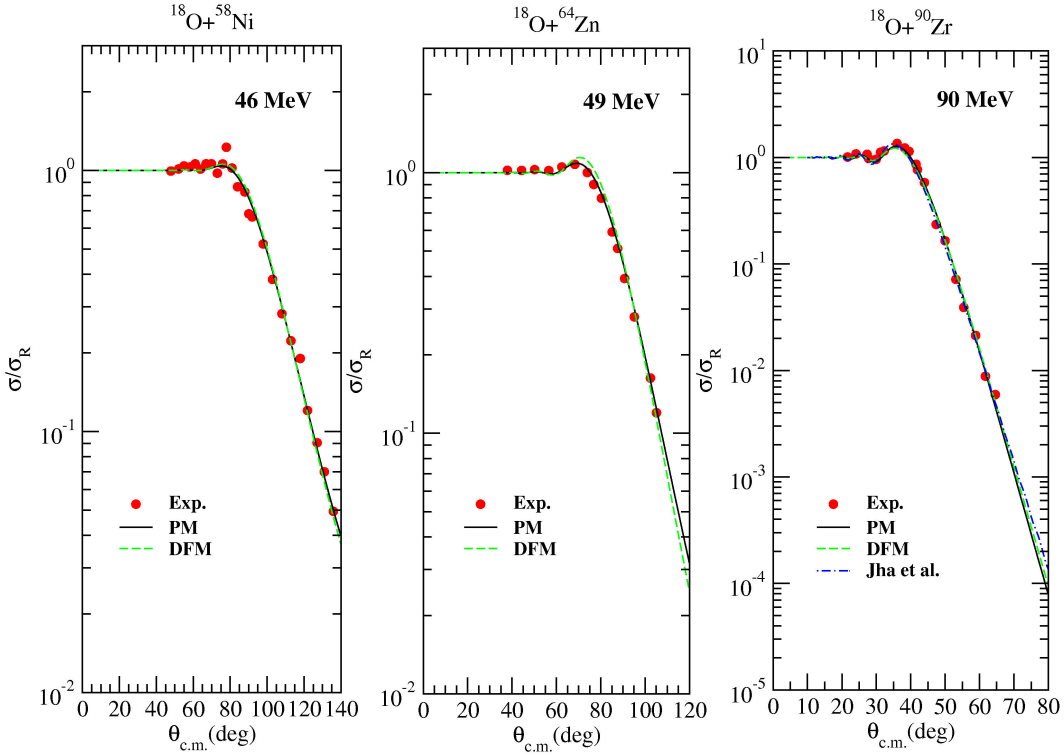

FIGURE 3. The elastic scattering angular distributions for ^{18}O + ^{58}Ni, ^{64}Zn and ^{90}Zr. The solid lines show PM results; dashed lines show DFM results and dot-dashed lines show the results obtained by the literature [16]. The circles show the experimental data, which have been taken from [14–16].

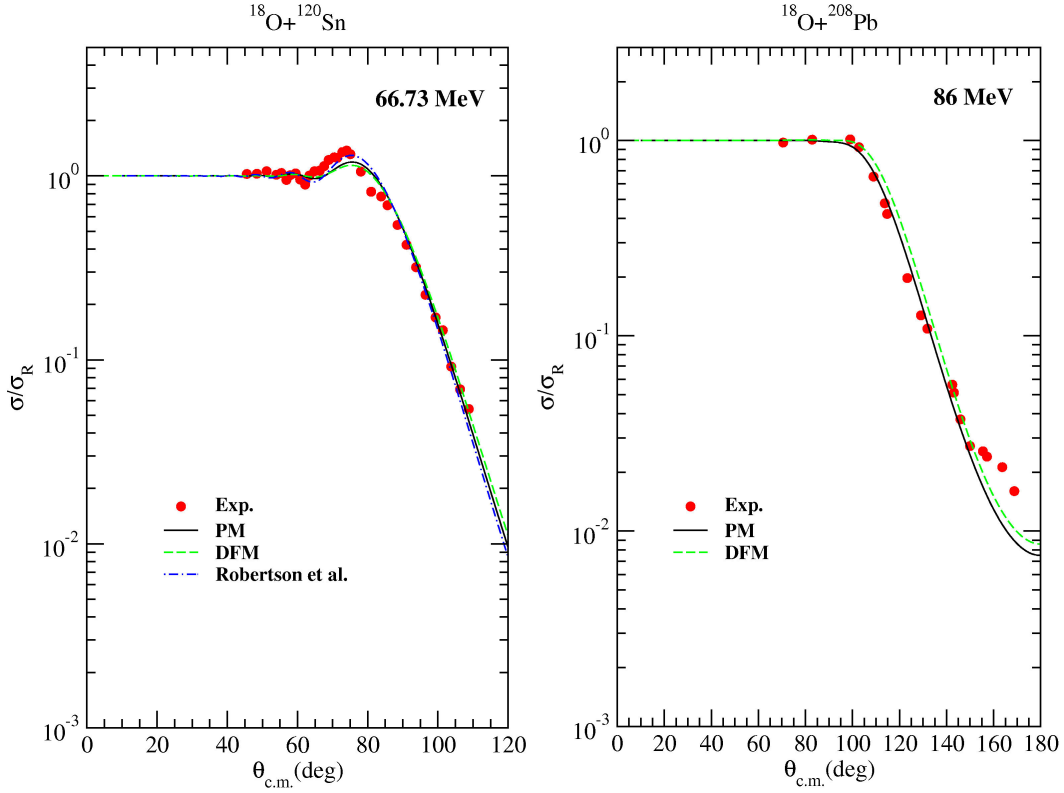

FIGURE 4. The elastic scattering angular distributions for ^{18}O + ^{120}Sn and ^{208}Pb. The solid lines show PM results; dashed lines show DFM results and dot-dashed lines show the results obtained by the literature [17]. The circles show the experimental data, which have been taken from [17, 18].

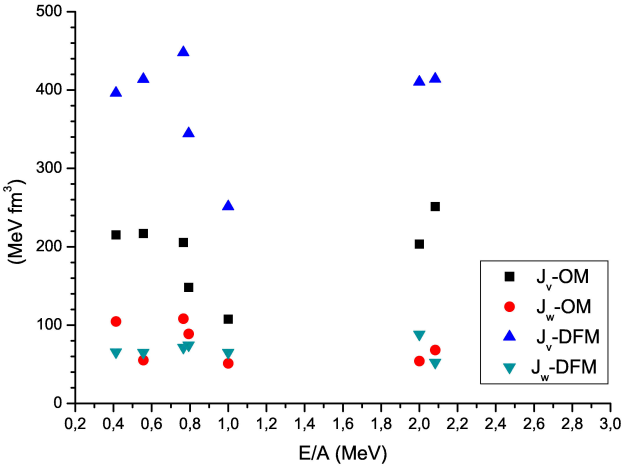

FIGURE 5. The real and imaginary volume integrals per interacting ion pair as a function of projectile energy per nucleon for seven different systems by means of the PM and the DFM.

imaginary volume integrals of the PM and the DFM potentials show very close values with each other.

In Tables I and II, we have given the cross-sections of all the systems examined by using the PM and the DFM. We have noticed that the cross-section values of both the PM and the DFM are very close to each other. As known from previous study [23], it can be said that similar cross-sections obtained for different OM calculations such as the PM and the DFM denote to good fits of the elastic scattering angular distributions. In this sense, we have compared our cross-sections with the literature. Bernas *et al*. [12] reported as 1314 mb the cross-section value of ^{18}O + ^{24}Mg reaction. For the cross-section of this system, we have obtained 1242.9 mb with the PM and 1182.8 mb with the DFM. Jha *et al*. [16] showed that the value of cross-section of ^{18}O + ^{90}Zr reaction has become 1500 mb. In our results, we have found 1504.6 mb with the PM and 1567.2 mb with the DFM for this system. The cross-sections which are close with each other can be attributed to the suitability of the fits of the elastic scattering angular distributions.

We have calculated the χ^2/N values for each system, which are given in Table I for the PM and in Table II for the DFM. We have noticed that χ^2/N values found via both models are generally very low. Hence, we can say that the theoretical results obtained for the PM and the DFM according to χ^2/N values are quite reasonable for the analysis of ^{18}O-target nucleus systems.

In our study, we have derived a new global set for the imaginary potential which depends on the incident energy of ^{18}O and the charge number(Z_T) and mass number(A_T) of target nuclei in order to use in the double folding calculations. With this goal, we have used the values in Table II obtained from the theoretical calculations of present study. Thus, this new equation is given as in the following form:

$$W = 16.88 - 0.075E + 3.783\frac{Z_T}{A_T^{1/3}}, \qquad (13)$$

where E is the incident energy of ^{18}O. We have obtained very close results to the values of Table II when this equation has been applied to find the depth of imaginary potential. However, this consistency is slightly disrupted for light target nuclei ^{24}Mg and ^{28}Si. We should draw attention that we do not aim to achieve the best fits for the experimental data. We try to derive a new global set for the imaginary potential which gives reasonable results with the experimental data. Consequently, we should say that this new equation can be used in the analysis of interactions of ^{18}O with different target nuclei, especially in the medium-heavy and heavy target nuclei.

4. Summary and Conclusions

We have introduced a global PM and DFM analysis of the elastic scattering angular distribution of ^{18}O by different target nuclei such as ^{24}Mg, ^{28}Si, ^{58}Ni, ^{64}Zn, ^{90}Zr, ^{120}Sn, and ^{208}Pb. To obtain the global potential sets, we have applied these methods to the systems. We have provided all the values of optical potential parameters obtained in Tables I and II. In addition to this, we have given the cross-sections and the volume integrals of all the reactions investigated. We have showed the theoretical results of the PM and the DFM as compared with the previous studies as well as the experimental data. We have observed that the PM and the DFM results are very compatible with each other. Also, these results of the PM and the DFM are in very good agreement with the experimental data. We have proposed a new global set for the imaginary potential to use in the double folding calculations. We have observed that the reasonable results with the experimental data for this new equation can be obtained.

Consequently, the theoretical results obtained with this study will be very useful and practical in calculations of elastic scattering, inelastic scattering, transfer reactions etc., of unknown reaction and energies of ^{18}O nucleus.

1. M. Aygun, *Commun. Theor. Phys.* **60** (2013) 69-72.
2. M. Aygun and I. Boztosun, *Few-Body Syst.* **55** (2014) 203-209.
3. M. Aygun, *Acta Phys. Pol. B* **45** (2014) 1875.
4. M. Aygun, I. Boztosun and Y. Sahin, *Phys. At. Nucl.* **75** (2012) 963-968.
5. M. Aygun, Y. Kucuk, I. Boztosun, and Awad A. Ibraheem, *Nucl. Phys. A* **848** (2010) 245-259.
6. R.F. Simões *et al.*, *Phys. Lett. B* **527** (2002) 187-192.
7. D.S. Monteiro *et al.*, *Nucl. Phys. A* **725** (2003) 60-68.
8. R.N. Sagaidak *et al.*, *Phys. Rev. C* **76** (2007) 034605.
9. A.T. Rudchik *et al.*, *Nucl. Phys. A* **860** (2011) 8-21.

10. A.T. Rudchik *et al., Nucl. Phys. A* **927** (2014) 209-219.
11. T.K. Steinbach *et al., Phys. Rev. C* **90** (2014) 041603(R).
12. M. Bernas *et al., Phys. Rev. C* **22** (1980) 1872.
13. M.C. Mermaz *et al., Phys. Rev. C* **19** (1979) 794.
14. J.J.S. Alves *et al., Nucl. Phys. A* **748** (2005) 59-74.
15. S. Salém-Vasconcelos *et al., Phys. Rev. C* **50** (1994) 927.
16. V. Jha, B.J. Roy, A. Chatterjee and H. Machner, *Eur. Phys. J. A* **19** (2004) 347-354.
17. B.C. Robertson *et al., Phys. Rev. C* **4** (1971) 2176.
18. E. Vulgaris, L. Grodzins, S.G. Steadman and R. Ledoux, *Phys. Rev. C* **33** (1986) 2017.
19. G.R. Satchler, Direct Nuclear Reactions (Oxford University Press, Oxford,1983).
20. Reference Input Parameter Library (RIPL-3), http://www-nds.iaea.org/RIPL-3/.
21. D.T. Khoa, G.R. Satchler and W. von Oertzen, *Phys. Rev. C* **51** (1995) 2069.
22. I.J. Thompson, *Computer Phys. Rep.* **7** (1988) 167.
23. M. Aygun, *Eur. Phys. J. A* **48** (2012) 145.